Comparison between MODIS aerosol product C004 and C005 and evaluation of their applicability in the north of China

ZHOU Chun-yan[1,2], LIU Qin-huo[1], TANG Yong[1], WANG Kai[1], SUN Lin[3], HE Ying-xia[4]

1. *State Key Laboratory of Remote Sensing Science*, *Jointly Sponsored by the Institute of oRemote Sensing Applications of Chinese Academy of Sciences and Beijing Normal University*, *Beijing* 100101, *China*;
2. *Satellite Environmental Application Center*, *Ministry of Environmental Protection of China*, *Beijing* 100029, *China*;
3. *Geomatics College*, *Shandong University of Science and Technology*, *Shandong Qingdao* 266510, *China*;
4. *LinYi Environmental Monitoring Station*, *Shandong Linyi* 276000, *China*

Abstract: MODIS aerosol product Collection 005 (C005) is an upgrade of C004, and is introduced in detail in this paper. Through fitting with AERONET ground observation aerosol optical thickness (AOT), MODIS aerosol C004 and C005 products of TERRA and AQUA are compared and evaluated to analyze their applicability in the north of China at Beijing and Yulin sites. We match AERONET ground-based data with MODIS aerosol product by band interpolation and temporal-spatial matching, then compare and evaluate them by linear fitting. We conceive a scale of temporal-spatial matching in the north of China considering the local aerosol movement velocity of given sites. The results show that: (1) C005 product algorithm does not improve the accuracy of AOT at Beijing site, and the accuracy drops when AOT< 0.8; both C004 and C005 products do not have a significant application at Beijing site, but the C004 performs better than C005 products. (2) At Yulin site, TERRA-MODIS C004 product meets the demand, and the accuracy of AQUA-MODIS C004 product decreases. Compared with the C004 product, the accuracy of the C005 product improves greatly, and correlation coefficients between AOTs of three bands (470nm, 550nm, 660nm) and the AERONET ground observation data are all higher than 0.9. It could be concluded that the method of the surface reflectance determination used in the new algorithm is feasible for dark dense vegetation, but is not suitable for the bright surface.

Key words: MODIS, C005, AERONET, aerosol optical thickness (AOT), validation

CLC number: P407 **Document code:** A

1 INTRODUCTION

Aerosol is a multiphase system composed of gas, solid and liquid particles suspended in air (Sheng *et al*., 2003). Aerosol originates from both man-made and natural sources. The man-made source aerosol is produced by human activities, such as burning fossil fuels, industrial and agricultural production activities; natural source aerosol is produced by natural phenomena, and can be directly emitted as particles into the atmosphere by forest fires, volcanic eruptions, sea spray, and the wind lifting dust particles in arid regions. Aerosol is one of important components of atmosphere, with characteristics of distributing widely, having short life span, moving rapidly, having complex chemical composition, etc. It plays an important role on climate change of whole world and region, and environment quality. It has become an important domain in the atmospheric science (Houghton *et al*., 1995; Anderson *et al*., 2003).

At present, there are two means of detecting aerosol: ground-based observations and satellite remote sensing. The former could provide exact aerosol optical thickness (AOT) for one point of space, but could not observe extensively because of the limitations of observation condition and instrument. The latter overcomes the shortcoming of ground observation. Thus, it could provide global aerosol characteristics. To retrieve aerosol by remote sensing began in 1970s. A series of satellite observation plans had been implemented, such as NOAA/AVHRR (Rao *et al*., 1989), TOMS (Herman *et al*., 1997), ATSR-2 (Veefkind *et al*., 2000), POLDER (Deuze *et al*., 1993), MODIS (Kaufman *et al*., 1997a), etc. These plans aimed at obtaining worldwide distribution of aerosol optical characteristic, seasonal and annual variation of aerosol direct and indirect force.

MODIS is the Moderate Resolution Imaging Spectroradiometer aboard Terra (EOS AM) and Aqua (EOS PM) satellites. MODIS acquires data globally in 36 spectral bands ranging in wavelength from 0.4 μm to 14.4μm. MODIS is the first satellite observation plan designed to provide aerosol optical characteristic globally of high spatial-resolution. It has been widely used

Received: 2008-04-14; **Accepted**: 2008-05-14

Foundation: Knowledge Innovation Engineering Project of CAS (No. KZCX2-YW-313) and National Natural Science Foundation of China (NSFC 40730525).

First author biography: ZHOU Chun-yan (1981—), female. She got Ph D in the Institute of Remote Sensing Applications, Chinese Academy of Sciences in July 2009, and did some researches about retrieving atmospheric aerosol and water vapor from remote sensing image. E-mail: mezhouchunyan@126.com

Corresponding Author: LIU Qin-huo (1968—), male, researcher and PhD supervisor. E-mail: qhliu@irsa.ac.cn

(C)1994-2021 China Academic Journal Electronic Publishing House. All rights reserved. http://www.cnki.net

to compute climate model, analyze dynamic change of environmental pollution, and monitor air quality in the global scope (Ichoku *et al*., 2004). During the past ten years, MODIS aerosol product algorithm had experienced modifications for many times. In 2006, collection 005 was introduced as the latest version of aerosol product to replace the Collection 004 (Levy *et al*., 2007). In recent years, a growing number of researchers began to study aerosol characteristic of China using MODIS aerosol product, and it is the basic research to evaluate MODIS aerosol product using ground observation. Mao *et al*. (2002) validated MODIS aerosol product of Beijing area using ground observation of Peking University. He found the nearest pixel from the ground site, which is within 15km away, then compared the pixel value with the arithmetical average of ground sun photometer observation in an hour. Due to the limitations of ground-based observations, timing differences between the two occur. So, the validation process requires temporal and spatial matching. Li *et al*. (2003) evaluated and confirmed TERRA-MODIS aerosol product of Beijing and Hong Kong areas using ground observations of two sites, and then studied aerosol optical characteristic and seasonal variation characteristic of the eastern China area using MODIS aerosol product. Xia (2006) contrasted AERONET AOT and MODIS aerosol product over land, and concluded that MODIS aerosol product overestimated AOT in most parts of the world. Wang *et al*. (2007) evaluated the applicability of MODIS aerosol product in different ecology types and geography regions of China using Chinese Sun Hazemeter Network (CSHNET). Mi *et al*. (2007) evaluated MODIS aerosol product in China using ground observations of Xianghe and Tai Lake sites. Li *et al*., (2003) Xia (2006), Wang *et al*. (2007), Mi *et al*. (2007) as mentioned above, all adopted the validation method provided by NASA to evaluate the MODIS aerosol product globally over land. The method is to match the version 2 AERONET AOT data within ±30 min of MODIS overpass times with MODIS retrieved AOT over a 50km×50km area centered on the AERONET sites. This method is designed for the global scale, and as such is not suitable for the local regions. This article will give full consideration to the velocity of aerosol in China, evaluate and discuss the applicability of old and new versions of MODIS aerosol products in the north China with AERONET ground observation data.

2 ALGORITHM OF MODIS AEROSOL PRODUCT C005 OVER LAND

So for, TERRA-MODIS aerosol product has been upgraded for 4 times: Collection 002, 003, 004, 005 (C002, C003, C004, C005 for short). C002 is the first version of the operational product, and is mainly applied in validation and analysis, and has not been widely used. C003 and C004 products have been released and are widely used. AUQU-MODIS aerosol product has been updated for 3 times: Collection 003, 004, 005, and the algorithm is similar to that of the same version of TERRA, but some minor complements (Levy *et al*., 2007). MODIS aerosol product C005 was released in the latter half year of 2006, and made a great improvement to the algorithm of C004 (Levy *et al*., 2007; Ichoku, 2005). This article will introduce the important improvements of C005 aerosol products algorithm from the following three aspects.

2.1 Change of inversion idea

The C004 algorithm assumes that aerosol is transparent in the 2.12μm channel, and surface reflectances in the visible channels are constant ratios to the observed reflectance (equal to surface reflectance) in 2.12μm. The C005 algorithm does not hold on this assumption, for many studies show that the 2.12μm channel contains information of coarse mode aerosol as well as the surface reflectance (Levy *et al*., 2007).

The C004 algorithm adopts the assumption proposed by Kaufman *et al*. (1997b) that over vegetated and dark soiled surfaces, the surface reflectances in some visible channels correlate with the surface reflectance in the SWIR. That is, surface reflectances in 0.47um (channel 3) and 0.66μm (channel 1) are assumed to be one-quarter and one-half of the surface reflectance in SWIR 2.12um (channel 7) respectively (Kaufman *et al*., 1997b). Later, many researches found that the VIS/SWIR surface ratios vary as a function of scattering geometry, and do not meet the relationship proposed by Kaufman *et al*. (1997b) under certain geometries (Remer *et al*., 2001; Gatebe *et al*., 2001). Therefore, these relationships between visible bands and SWIR band are completely broken. The C005 algorithm adopts a new assumption: over dark surfaces, the RED/SWIR surface ratio varies as a function of scattering angle and vegetation index, and the RED/BLUE surface ratio is assumed to be fixed. As follows (Levy *et al*., 2007):

$$\rho^{s}_{0.66} = f(\rho^{s}_{2.12}) = \rho^{s}_{2.12} \times \mathrm{slope}_{0.66/2.12} + \mathrm{yint}_{0.66/2.12}$$

$$\rho^{s}_{0.47} = f(\rho^{s}_{0.66}) = \rho^{s}_{0.66} \times \mathrm{slope}_{0.47/0.66} + \mathrm{yint}_{0.47/0.66}$$

where

$$\mathrm{slope}_{0.66/2.12} = \mathrm{slope}^{\mathrm{NDVI_{SWIR}}}_{0.66/2.12} + 0.002\Theta - 0.27,$$

$$\mathrm{yint}_{0.66/2.12} = -0.00025\Theta + 0.033,$$

$$\mathrm{slope}_{0.47/0.66} = 0.49,$$

$$\mathrm{yint}_{0.47/0.66} = 0.005.$$

$$\mathrm{slope}^{\mathrm{NDVI_{SWIR}}}_{0.66/2.12} = 0.48;\ \mathrm{NDVI_{SWIR}} < 0.25,$$

$$\mathrm{slope}^{\mathrm{NDVI_{SWIR}}}_{0.66/2.12} = 0.58;\ \mathrm{NDVI_{SWIR}} > 0.75,$$

$$\mathrm{slope}^{\mathrm{NDVI_{SWIR}}}_{0.66/2.12} = 0.48 + 0.2(\mathrm{NDVI_{SWIR}} - 0.25);\quad 0.25 \leqslant \mathrm{NDVI_{SWIR}} \leqslant 0.75.$$

$$\mathrm{NDVI_{SWIR}} = (\rho^{m}_{1.24} - \rho^{m}_{2.12})/(\rho^{m}_{1.24} + \rho^{m}_{2.12}).$$

$\rho^{s}_{0.66}$, $\rho^{s}_{0.47}$, $\rho^{s}_{2.12}$ represent the surface reflectance in 0.66μm, 0.47μm, 2.12μm, respectively; $\rho^{m}_{1.24}$, $\rho^{m}_{2.12}$ represent the measured surface reflectance in 1.24μm, 2.12μm respectively; Θ is the scattering angle.

2.2 Change of radiative transfer code

The C004 MODIS lookup table (LUT) is calculated using

(C)1994-2021 China Academic Journal Electronic Publishing House. All rights reserved. http://www.cnki.net

the non-polarized (scalar) SPD radiative transfer (RT) code (Dave *et al*., 1970). Fraser *et al*. in 1992 and Levy *et al*. in 2004 found that under some observation conditions, the neglect of the polarization scattering information would lead to significant errors in top of atmosphere reflectance. The algorithm chooses RT3 (Evans & Stephens, 1991), a vector RT code, to calculate the C005 MODIS lookup table (LUT). RT3 runs in scalar and vector modes, in order to keep joined with the former version. It is combined with MIEV (Wiscombe, 1981) for spherical fine aerosol and T-matrix (Dubovik *et al*., 2002a) for the non-spherical coarse aerosol to calculate the scattering properties of models (Levy *et al*., 2007).

2.3 Change of aerosol model

The C005 algorithm defines the aerosol models according to the geographical distribution. Five kinds of aerosol models: continental, dust, non-absorbing, neutral absorbing, and highly absorbing, are defined by slightly modifying the result of Dubovik *et al*.'s research (2002b). They are quite different from those in previous versions which were defined according to the research done by Remer *et al*. in 1998. Continental aerosol model is used only over bright surface; non-absorbing, neutral absorbing, and highly absorbing aerosol models are all fine models, which change with seasons and geographical locations; C005 algorithm defines a combination aerosol model by choosing dust model and one of those fine models (Levy *et al*., 2007).

The C005 algorithm redefines aerosol optical characteristic according to AERONET, especially for single scattering albedo (SSA): SSA~0.95 for the non-absorbing model, SSA~0.90 for the neutral absorbing model, and SSA~0.85 for the highly absorbing model (Levy *et al*., 2007). In China, except for the eastern coast, most areas are defined as neutral absorbing model. Over the past few years, so sparse the sites of AERONET in China there are that aerosol optical characteristics were not sufficiently studied. With the ground-based observations of aerosols in China being increasing in recent years, AERONET sites in China have increased significantly, while many provincial and municipal institutions have begun to observe on their own. Institute of Atmospheric Physics, Chinese Academy of Sciences, establishes the Chinese Sun Hazemeter Network, which currently has 19 ecology observation sites of Chinese Ecosystem Research Network, 4 urban observation sites, 2 calibration centers and 1 data center. Institute of Remote Sensing Application, Chinese Academy of Sciences, set a CE318 sun photometer on the roof of the institute building, to monitor the atmosphere condition around the Olympic venues during the Olympic Games in 2008. Hebei, Shanxi and many other provinces have begun to use CE318 sun photometer to observe aerosol. It is believed that in the next few years, there will be a more detailed and accurate description of aerosol characteristics of China.

Some other modifications are also done in the C005 algorithm, such as the choice of dark target, cloud mask, snow mask, the definition of the center wavelength, elevation correction, etc. These would not be expatiated in this paper, please refer to relevant literatures if interested (Levy *et al*., 2007).

3 DESIGN THE VALIDATION SCHEME FOR MODIS AEROSOL PRODUCT IN CHINA

3.1 Preparation of data

TERRA\AQUA-MODIS aerosol C004 and C005 products from August 28 to October 8 in 2002 covering the north of China are adopted in this paper, AERONET aerosol data of Beijing and Yulin sites of the same time in northern China are also chosen. MODIS C004 and C005 products of TERRA and AQUA are validated by these two AERONET sites.

AErosol RObotic NETwork (AERONET) program provides globally distributed observations of spectral aerosol optical characteristic in representative regions, for global aerosol transmission and radiative research, validation of radiative transfer model and satellite retrievals. The AERONET program is a federation of ground-based remote sensing aerosol networks with vast observation sites all over the world. The whole network uses multi-band sun photometer of CIMEL Company, France. The network imposes standardization of instruments, calibration, processing and distribution. The observation data possesses fine accuracy, and thus, are now widely applied to verify the accuracy of spectral aerosol optical characteristic achieved by other methods. AOT data are computed for three data quality levels: Level 1.0 (unscreened), Level 1.5 (cloud-screened), and Level 2.0 (cloud-screened and quality-assured) (Holben *et al*., 1998). Level 2.0 AERONET AOT data is adopted to validate MODIS aerosol product in this paper.

3.2 Methods of data matching

MODIS aerosol products and AERONET aerosol observations have different center wavelengths and temporal and spatial resolutions. Thus, band interpolation and spatial-temporal matching processing should be done to AOT in order to make it feasible to compare these two kinds of AOT data reasonably (Chen *et al*., 2005).

3.2.1 Band interpolation

AERONET sun photometers usually derive AOT in 340, 380, 440, 500, 670, 870, and 1020 nm wavelengths from direct solar radiation measurements, while MODIS aerosol algorithm routinely retrieves AOT in 470 and 660nm wavelengths (and interpolates in 550 nm) over land surfaces. AERONET and MODIS wavelengths do not match exactly. Therefore, interpolation of AERONET AOT is needed to be done to enable the comparison, AERONET AOT in 470, 550, and 660nm are interpolated from AERONET AOT in 440 and 870 nm based on the assumption of uniform spectral dependence between these two wavelengths. The data in 500nm is not taken into interpolation for the sake of the universality of the algorithm. Not all the AERONET sites are able to get the data in this band.

(C)1994-2021 China Academic Journal Electronic Publishing House. All rights reserved. http://www.cnki.net

AERONET offers observation in 670nm, which is close to the band of 660nm of MODIS. In order to ensure the observation in 670nm is independent of the accidental calibration error as those in the other two bands do, the data in 660nm for AERONET is calculated by interpolation of those two bands in this paper (Fraser *et al*., 1992; Remer *et al*., 2005).

In the band with no influence of water vapor, the size distribution of aerosol particles fits Junge-distribution, and the relation of AOT and wavelength fits the Angstrom function (Angstrom, 1964):

$$\tau_a(\lambda) = \beta\lambda^{-\alpha}$$

where, $\tau_a(\lambda)$ represents AOT in the band of λ; β represents Angstrom turbidity, which is related with aerosol particle quantity, particle size distribution, and refraction coefficient; α represents Angstrom wavelength, which is related to the average radius of aerosol particles, ranging in [0,4]. The larger the aerosol particle is, the smaller the value is.

Assuming there are no influence of water vapor in the bands of λ_1 and λ_2 then:

$$\tau_a(\lambda_1) = \beta\lambda_1^{-\alpha}$$

$$\tau_a(\lambda_2) = \beta\lambda_2^{-\alpha}$$

Therefore:

$$\alpha_{870/440} = -\frac{\ln(\tau_a(870)/\tau_a(440))}{\ln(870/440)}$$

Then, the AOT in the bands of 470, 550nm and 660nm could be calculated by the following equation respectively:

$$\tau_a(\lambda) = \tau_a(870)(\lambda/870)^{-\alpha_{870/440}}$$

The error of interpolation is between 0% and 10%, and depends on the types of aerosol models. The error is larger when the fine mode is in the dominant place and the AOT is large; while the error is smaller if the aerosol model is mixed or coarse mode (Eck *et al*., 1999).

3.2.2 Temporal and spatial matching processing of MODIS aerosol product and AERONET observation

AERONET AOT is acquired at 15-minute intervals on average on some instrumented locations, while MODIS could provide aerosol spatial distribution of a fixed time with a pixel size of 10km×10km. The MODIS aerosol product of TERRA and AQUA are chosen. The satellite passing time is around 10:30 AM locally for TERRA and 1:30 PM for AQUA. The aerosol observations of MODIS and AERONET are different in temporal and spatial scales. If simply comparing the AOT of AERONET at the time of MODIS passing and that of a single pixel of MODIS covering the site, which is actually a comparison of the AOT at one point and the average AOT in the region of 10km×10km, no persuasive conclusion could be achieved. Therefore, another stable and reliable matching processing is required. At present, NASA and many researchers adopt a matching method for MODIS aerosol product proposed by Ichoku *et al*. (2002). They thought that the level 2.0 AERONET AOT within ±30 min of MODIS overpass times were matched with MODIS retrieved AOT over a 50km×50 km area centered on the AERONET sites. The equivalence described by Ichoku *et al*. (2002) is based on the assumption that, air masses transporting aerosol travel a distance of approximately 50 km per hour on average by estimates of Saharan dust transport. It is not the case in the local scale.

The velocities of aerosol spatial movement in different region are different, and are influenced by many factors, such as wind in horizontal direction and onflow in the vertical direction. In this paper, only the movement in horizontal direction is taken into account. The month average wind velocity of Beijing and Yulin sites from 1971 to 2000, shown in Table 1, is collected from the climate background statistical data supplied by China Meteorological Data Sharing Service System (CMDSSS). Taking Beijing site for example, the wind velocity of these three months differs little. The data of September is chosen, considering most of MODIS aerosol products used in this paper are in this month. The wind velocity is 7.2km/h. As wind is the carrier of aerosol in the horizontal direction, it is supposed that the velocity of aerosol movement is the same with the wind speed in the horizontal direction. The aerosol moving velocity is regarded as 7.2km/h for Beijing, and 6.48km/h for Yulin. The pixel size of MODIS aerosol product is 10km×10km. Therefore, we will match AERONET data within ±30 min of MODIS overpass time with a pixel of MODIS aerosol product covering the AERONET sites.

Table 1 Month average wind velocity of study sites/(m/s)

Site \ Month	August	September	October
Beijing	1.8	2.0	2.1
Yulin	2.2	1.8	1.8

3.3 Validation method

After band interpolation of AERONET data and spatial-temporal matching processing of MODIS data, a linear fitting analysis is to be done for these two data.

$$\tau_{\mathrm{MODIS}} = A\tau_{\mathrm{AERONET}} + B$$

where, τ_{MODIS} is the retrieved AOT of MODIS, A is the slope, τ_{AERONET} is the observed AOT of AERONET, B is the intercept.

Under ideal condition, the retrieved AOT of MODIS should be equal to the observed AOT of AERONET, that is: A=1, B=0, correlation coefficient R=1. However, due to the error resulted from sun photometer itself, band interpolation, spatial-temporal matching processing, and especially MODIS aerosol retrieval, these two data are not equal. In this paper, the accuracy of AOT of MODIS is evaluated by the linear correlation coefficient R, slope A, intercept B, and percentages of MODIS AOT falling within the specified uncertainty bounds as shown in Table 2 and Table 3.

(C)1994-2021 China Academic Journal Electronic Publishing House. All rights reserved. http://www.cnki.net

4 RESULTS AND ANALYSIS

As shown in Fig.1 and Fig. 2, there are the linear fitting results between TERRA\AQUA MODIS AOT and AERONET ground observation AOT in 470nm, 550nm, 660nm three bands at Beijing and Yulin sites. The X-axel is the observed AOT of AERONET, and the Y-axel is the retrieved AOT of MODIS. The expectation error range of MODIS aerosol product defined by NASA is adopted in this paper, which is: $\tau = \pm 0.05 \pm 0.15 \tau_{\mathrm{AERONET}}$ (Remer *et al*., 2005). The linear fitting function and correlation coefficient (R) are presented in Fig.1 and Fig. 2.

As shown in the left of Fig. 1, there are the linear fitting results between TERRA-MODIS AOT and AERONET ground observation AOT in 470nm, 550nm, 660nm three bands at Beijing site. Among all the TERRA-MODIS C004 and C005 products at Beijing site used in the paper, there are 26 valid

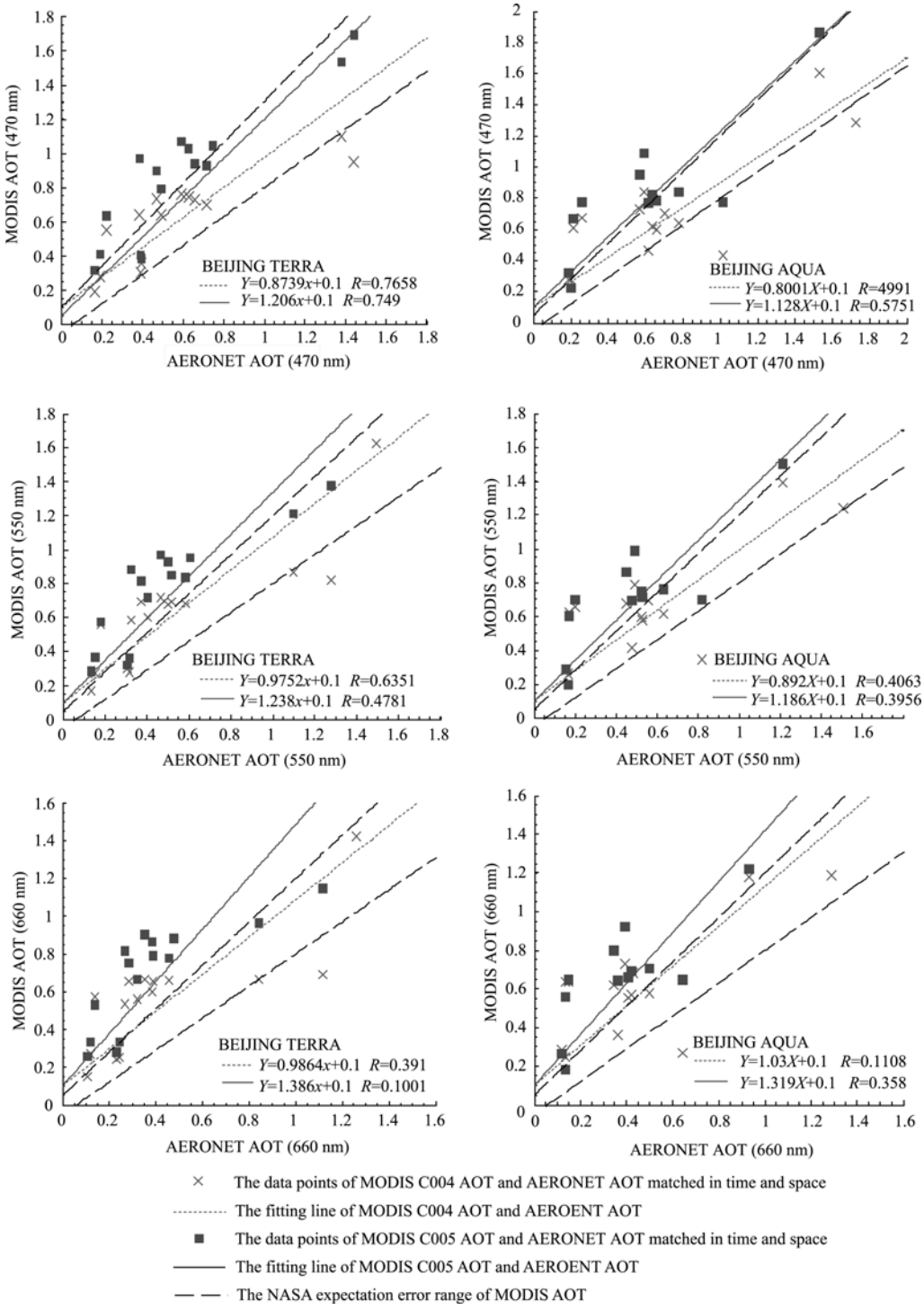

Fig. 1 Linear fitting between TERRA (left), AQUA (right) MODIS AOT and AERONET ground observation AOT in 470nm (upper), 550nm (middle), 660nm (lower) three bands at Beijing site

(C)1994-2021 China Academic Journal Electronic Publishing House. All rights reserved. http://www.cnki.net

Table 2 The probability statistics of TERRA, AQUA MODIS AOT falling into the NASA expectation error range at Beijing site

Band	470nm		550nm		660nm	
Product	C004	C005	C004	C005	C004	C005
TERRA/%	46.7	26.7	33.3	26.7	26.7	20.0
AQUA/%	42.9	25.0	42.9	25.0	21.4	16.7

values for each, but only 15 of them could match with the AERONET ground observation data. One of the key reasons for this limited matching data is the absence of ground observation at Beijing site from 1st to 7th Oct, 2002. After an intuitive analysis of the fitting in 470nm, 550nm, 660nm three bands, it should be noticed that: when AERONET AOT is less than 0.8, most of C004 AOT is lower than that of C005, and both C004 and C005 products obviously overestimate the actual AOT; when AERONET AOT is larger than 0.8, C004 product severely underestimates the actual value, while that of C005 is more closed to the actual value. In 470nm (as shown in the upper left of Fig. 1), for the linear fitting of C004, C005 MODIS aerosol products and AERONET AOT, the slopes are 0.8739 and 1.206, the intercept is 0.1 for both, and the correlation coefficients are 0.7658 and 0.749, percentages of sample falling into the NASA expectation error range are 46.7% and 26.7% (as shown in Table 2), respectively. All these data leads to the conclusion that the accuracy of C004 product is higher than that of C005 product in 470nm. Nevertheless, both these two products cannot achieve good fitting result of the actual value. The percentages of sample falling into the NASA expectation error range are also too low. Therefore, both products lack applicability at Beijing site. After analyzing the four factors: slope, intercept, correlation coefficient and percentage of sample falling into the NASA expectation error range, a similar conclusion with that in 470nm could be reached, that is: TERRA-MODIS C004 and C005 aerosol products in 550nm and 660nm do not perform well in Beijing, but the accuracy of C004 is higher than that of C005.

As shown in the right of Fig. 1, there are the linear fitting results between AQUA-MODIS AOT and AERONET ground observation AOT in 470nm, 550nm, 660nm three bands at Beijing site. It is used to omit AQUA-MODIS aerosol data in validating MODIS aerosol product. Passing time is around 1:30 pm locally for AQUA, at which AERONET data is rich. Therefore AQUA-MODIS aerosol product could lend strong support to the validation. Among all AQUA-MODIS aerosol C004 and C005 products at Beijing site used in the paper, there are 24 valid values for C004, but only 20 for C005. Limited valid value for C005 results from the stricter cloud screening of C005. After the temporal matching processing with the AERONET data, 14 valid values of C004 and 12 valid values of C005 are able to be applied to fitting. By looking through the fitting formula in the three bands as shown on the right of Fig. 1, it is concluded that the fitting effect of all is poor. All the intercepts are over 0.1, the slopes are far from 1, and the correlation coefficients are low in most bands except that 0.5751 in 470 nm for C005. Moreover, the percentages of sample falling into the NASA expectation error range are lower than those of TERRA. AQUA-MODIS aerosol product of Beijing site is not applicable, and is weaker than that of TERRA in accuracy. It must result from the systemic error of these two satellite systems.

Beijing site (39.977N, 116.381E) is located on a terrace on the roof of the Institute of Atmospheric Physics building. There are resident buildings, commercial buildings, roads, and scattering greenbelt other than vast green land around it. Thus, it is typical urban aerosol. TERRA\AQUA-MODIS aerosol C004 and C005 products are compared and evaluated through linear fitting with the AERONET ground observation AOT at Beijing site. The results show that both C004 and C005 products are lack of applicability, but the C004 performs better than C005; improvements of C005 product algorithm do not improve the accuracy of AOT at Beijing site, and accuracy drops when AOT< 0.8. There are notable difference between C005 aerosol product and the true value, and we think that it is caused by inaccurate reflectance retrieved by the algorithm of MODIS AOT over the bright surface. It still needs to look for the dark dense vegetation in the algorithm of MODIS C005 aerosol product. However, there is no large scale vegetation around the Beijing site. Data selected in this paper is during autumn, which makes it more difficult to find dark pixels. So there is no way to determine the ground reflectance accurately. Otherwise, urban aerosol almost originates from human being activities, whose characteristic is difficult to describe exactly. We think that it is an important factor influencing the accuracy of retrieved AOT. In a word, both of MODIS C004 and C005 products are not applicable over the bright surface.

As shown in the left of Fig. 2, there are the linear fitting results between TERRA-MODIS AOT and AERONET ground observation AOT in 470nm, 550nm, 660nm three bands at Yulin site. The total valid TERRA-MODIS AOT values at Yulin site are 26 and 18 for C004 and C005 respectively. After temporal matching with AERONET data, 25 and 17, of them could be applied to fitting respectively. In 470nm (as shown in the upper left of Fig. 2), the slope of C005 fitting is 0.9983, which is close to 1, and the correlation coefficient is 0.9447. Percentage of sample falling into the NASA expectation error range is up to 76.5% (as shown in Table 3). In short, C005 has higher accuracy than C004. In 550nm (as shown in the middle left of Fig. 2), the slope of C005 fitting is close to 1, the intercept is –0.056, and the correlation coefficient is 0.9366. Percentage of sample falling into the NASA expectation error range is 64.7%. C005 AOT in this band remains quite accurate as that in 470nm. The correlation coefficient of C004 is rather lower, and the intercept is as large as 0.1. However, percentage of sample falling into the NASA expectation error range is as

(C)1994-2021 China Academic Journal Electronic Publishing House. All rights reserved. http://www.cnki.net

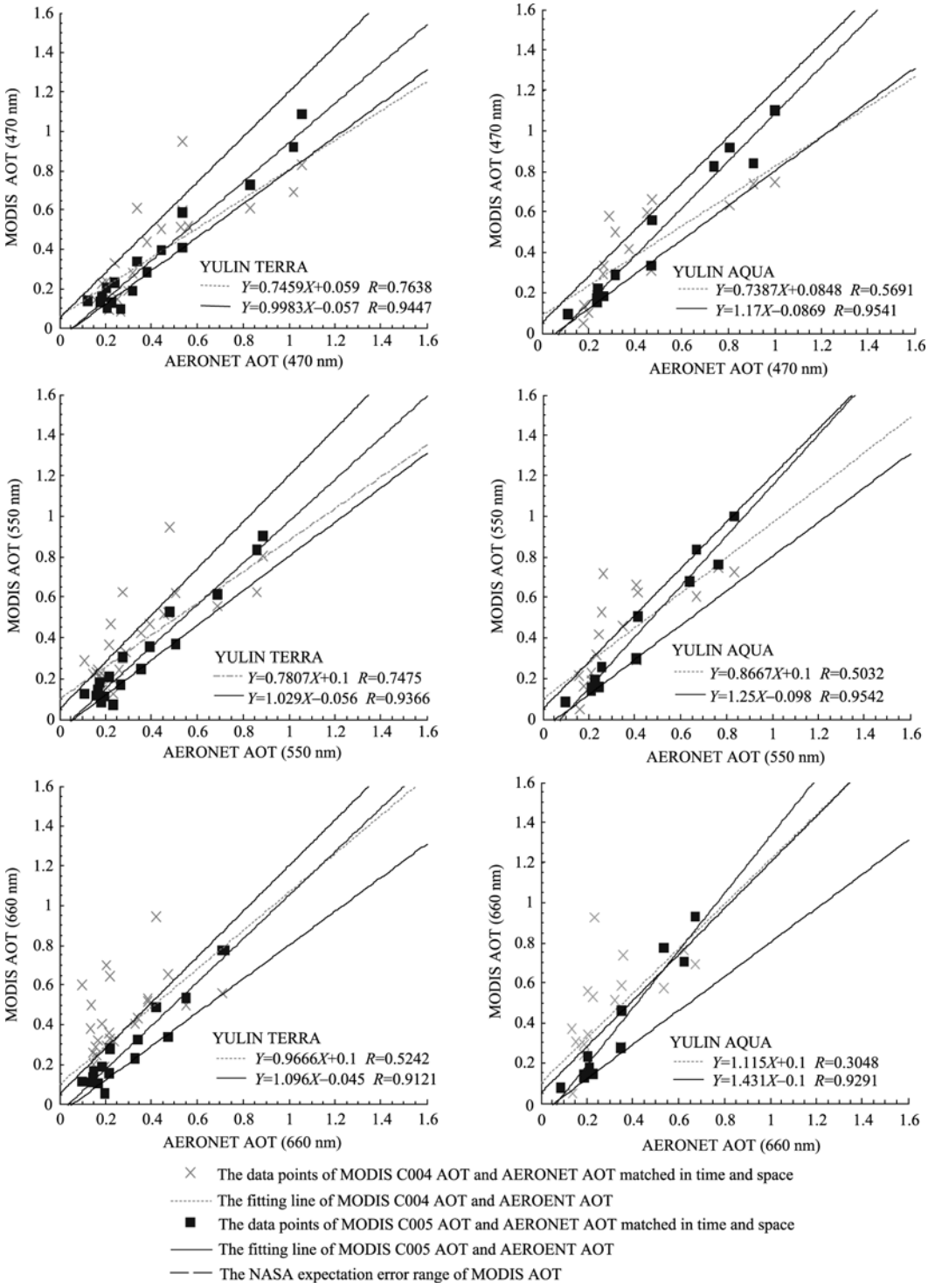

Fig. 2 Linear fitting between TERRA (left), AQUA (right) MODIS AOT and AERONET ground observation AOT in 470nm (upper), 550nm (middle), 660nm (lower) three bands at Yulin site

Table 3 The probability statistics of TERRA, AQUA MODIS AOT falling into the NASA expectation error range at Yulin site

Band	470nm		550nm		660nm	
Product	C004	C005	C004	C005	C004	C005
TERRA/%	52.0	76.5	68.0	64.7	32.0	87.5
AQUA/%	43.8	91.7	50.0	75.0	31.3	72.7

high as 68.0%. Both C004 and C005 products are highly reliable in this band. C005 product has higher accuracy than C004. In 660nm (as shown in the lower left of Fig. 2), for C005 product, the fitting results are also good, and percentage of sample

(C)1994-2021 China Academic Journal Electronic Publishing House. All rights reserved. http://www.cnki.net

falling into the NASA expectation error range is 87.5%. So the product is reliable. However for C004 product, the correlation coefficient drops to 0.5242, and percentage of sample falling into the NASA expectation error range is 32.0%. Thus, the accuracy declines sharply comparing to the other two bands. In conclusion, for C004 product, the accuracy in 470nm is the best, that in 500nm is less, and the 600nm is the least. The products in the first two bands are reliable. For C005, the accuracies in these three bands are close to each other, and are all in a high level. Thus, products all share the merit of applicability.

As shown in the right of Fig. 2, there are the linear fitting results between AQUA-MODIS AOT and AERONET ground observation AOT in 470nm, 550nm, 660nm three bands at Yulin site. After temporal matching with AERONET data, there are 16 and only 12 valid values for C004 and C005 products respectively. Considering the slope, intercept and correlation coefficient of the linear fitting equation and the percentages of sample falling into the NASA expectation error range (as shown in Table 3) in these three bands, it could be concluded that: for C005 product, its accuracy remains a level as high as that of TERRA product, but its slope becomes larger; for C004 product, the correlation coefficient decreases tremendously, and percentages of sample falling into the NASA expectation error range also decline. In Yulin area, the AQUA-MODIS C005 product has the merit of applicability.

Yulin site (38.283N, 109.717E) is located on a terrace on the roof of the Shaanxi Desert Institute in Yulin at an elevation of 1080 meters. There is strong blast of wind laden with sand in spring and plenty of rain in summer. In summer and fall, the vegetation cover is fine, and the weather condition is good. Through the comparison above, it is known that TERRA-MODIS aerosol product C004 could satisfy the requirement, while the accuracy of AQUA-MODIS aerosol product C004 is lower. For C005 product, both satellites perform well in accuracy, and also share the merit of applicability. The modification for method of determining land surface reflectance in C005 algorithms exerts tremendous influence in the region with fine vegetation cover. In this paper, the retrieved AOT at Yulin site is improved notably.

5 CONCLUSIONS

TERRA\AQUA-MODIS aerosol C004 and C005 products are compared and evaluated through fitting with the AERONET ground observation AOT at Beijing and Yulin sites in this paper. The results show that: (1) improvements of C005 product algorithm do not improve the accuracy of AOT at Beijing site, and the accuracy drops when AOT<0.8. Both C004 and C005 products do not have obvious applicability, but C004 product performs better than C005 product. (2) At Yulin site, TERRA-MODIS C004 product could satisfy the demands, but the accuracy of AQUA-MODIS C004 product drops slightly. The accuracy of C005 product improves greatly, and the correlation coefficients between AOTs of three bands (470nm, 550nm, 660nm) and the AERONET ground observation data are all higher than 0.9. Both C004 and C005 have obvious applicability. It shows that the method of the surface reflectance determination used in the new algorithm is feasible for dark dense vegetation area, but not suitable for the bright surface. In a word, TERRA\AQUA-MODIS aerosol C004 and C005 products all do not have obvious applicability over bright surface in the north of China; TERRA-MODIS C004 product has certain reliability over dark dense vegetation area, while AQUA-MODIS C004 product has lower accuracy than that of TERRA; C005 products of TERRA and AQUA all have high accuracy over dark dense vegetation area in the north of China, and show a good applicability.

There are various surface types in China, and thus there is more work to do in order to improve the accuracy of retrieved AOT. On one hand, it is necessary to accurately determine the reflectance of different types of land surface, such as dark dense vegetation, sparse vegetation, high reflectance surface and inner land lake. At present, though there is reliable model for dark dense vegetation surface, further research needs to be done for other land surface types. On the other hand, the aerosol characteristic could exert significant influence on the accuracy of product, including single scattering albedo, refraction index, size distribution, etc. With the development of ground-based observation, it is possible to describe the aerosol characteristic precisely, and as such to improve the accuracy of satellite remote sensing retrieving aerosol.

Acknowledgements: Thanks Dr. Song Yu in Peking University for his direction and help in aerosol movement. Thanks NASA GSFC for MODIS aerosol product data and AERONET ground-based data needed in this paper.

REFERENCES

Anderson T L, Charlson R J, Schwartz S E, Knutti R, Boucher O, Rodhe H and Heintzenberg J. 2003. Climate forcing by aerosols—a hazy picture. *Science*, **300**(5622): 1103—1104

Angstrom A. 1964. The parameters of atmospheric turbidity. *Tellus*, **16**: 64—75

Chen B Q and Yang Y M. 2005. Validation of MODIS aerosol optical thickness in the Taiwan Strait and its circumjacent sea area. *Acta Oceanologica Sinica*, **27**(6): 170—176

China Meteorological Administration.China Meteorological Data Sharing Service System. Ground observation. < http://cdc.cma.gov.cn/> (1 Mar, 2008)

Dave J V. 1970. Intensity and polarization of radiation emerging from a plane-parallel atmosphere containing mono-dispersed aerosols. *Applied Optics*, **9**(12): 2673—2687

Deuze J L, Breon F M, Deschamps P Y, Devaux C, Herman M, Podaire A and Roujean J L.1993. Analysis of the POLDER (Polarization and Directionality of Earth's Reflectances) airborne in-

(C)1994-2021 China Academic Journal Electronic Publishing House. All rights reserved. http://www.cnki.net

strument. *Remote Sensing of Environment*, **45**(2): 137—154

Dubovik O, Holben B N, Lapyonok T, Sinyuk A, Mishchenko M I, Yang P and Slutsker I. 2002a. Non-spherical aerosol retrieval method employing light scattering by spheroids. *Geophysical Research Letters*, **29**(10): 1415, doi:10.1029/2001GL014506

Dubovik O, Holben B N, Eck T F, Smirnov A, Kaufman Y J, King M D, Tanré D and Slutsker I. 2002b. Variability of absorption and optical properties of key aerosol types observed in worldwide locations. *Journal of the Atmospheric Sciences*, **59**(3): 590—608

Eck T F, Holben B N, Reid J S, Dubovik O, Smirnov A, O'Neill N T, Slutsker I and Kinne S. 1999. Wavelength dependence of the optical depth of biomass burning, urban and desert dust aerosols. *J. Geophys. Res.*, **104**(31): 331—350

Evans K F and Stephens G L. 1991. A new polarized atmospheric radiative transfer model. *Journal of Quantitative Spectroscopy and Radiative Transfer*, **46**(5): 413—423

Fraser R S, Ferrare R A, Kaufman Y J, Markham B L and Mattoo S. 1992. Algorithm for atmospheric corrections of aircraft and satellite imagery. *International Journal of Remote Sensing*, **13**(3): 541—557

Gatebe C K, King M D, Tsay S C, Ji Q, Arnold G T and Li J Y. 2001. Sensitivity of off-nadir zenith angles to correlation between visible and near-infrared reflectance for use in remote sensing of aerosol over land. *IEEE Transactions on Geoscience and Remote Sensing*, **39**(4): 805—819

Herman J R, Bhartia P K, Torres O, Hsu C, Seftor C and Celarier E. 1997. Global distribution of UV-absorbing aerosols from Nimbus 7/TOMS data. *J. Geophys. Res.*, **102**(D14): 16911—16922

Holben B N, Eck T F, Slutsker I, Tanré D, Buis J P, Setzer A, Vermote E, Reagan J A, Kaufman Y J, Nakajima T, Lavenu F, Jankowiak I and Smirnov A. 1998. AERONET-a federated instrument network and data archive for aerosol characterization. *Remote sensing of environment*, **66**(1): 1—16

Houghton J T, Meira Filho L G, Bruce J, Lee H, Callander B A, Haites E, Harris N and Maskell K. 1995. IPCC, Climate Change 1994: Radiative Forcing of Climate Change and an Evaluation of the IPCC IS92 Emission Scenarios. Cambridge: Cambridge University Press

Ichoku C, Chu D A, Mattoo S, Kaufman Y J, Remer L A, Tanré D, Slutsker I and Holben B N. 2002. A spatio-temporal approach for global validation and analysis of MODIS aerosol products. *Geophysical Research Letters*, **29**(12), 8006, doi: 10.1029/2001GL013206.

Ichoku C, Kaufman Y J, Remer L A and Levy R. 2004. Global aerosol remote sensing from MODIS. *Advances in Space Research*, **34**(4): 820—827

Ichoku C, Remer L A and Eck T F. 2005. Quantitative evaluation and intercomparison of morning and afternoon Moderate Resolution Imaging Spectroradiometer (MODIS) aerosol measurements from Terra and Aqua. *J. Geophys. Res.*, **110**, D10S03, doi: 10.1029/2004JD004987.

Kaufman Y J, Tanré D, Remer L A, Vermote E F, Chu A and Holben B N. 1997a. Operational remote sensing of tropospheric aerosol over land from EOS-Moderate Resolution Imaging Spectroradiometer. J. Geophys. Res, **102**(D14): 17051—17067

Kaufman Y J, Wald A E, Remer L A, Gao B C, Li R R and Flynn L. 1997b. The MODIS 2.1-um channel–correlation with visible reflectance for use in remote sensing of aerosol. *IEEE Transactions on Geoscience and Remote Sensing*, **35**(5): 1286—1298

Levy R C, Remer L A and Kaufman Y J. 2004. Effects of neglecting polarization on the MODIS aerosolretrieval over land. *IEEE Transactions on Geoscience and Remote Sensing*, **42**(11): 2576—2583

Levy R C, Remer L A, Mattoo S, Vermote E F and Kaufman Y J. 2007. Second-generation operational algorithm: Retrieval of aerosol properties over land from inversion of moderate resolution imaging spectroradiometer spectral reflectance. *J. Geophys. Res.*, **112**, D13211, doi: 10.1029/2006JD007811.

Li C C, Mao J T, Liu Q H, Chen J Z, Yuan Z B, Liu X Y, Zhu A H and Liu G Q. 2003. Study of distribution and the seasonal variation characteristic of aerosol optical thickness using MODIS in the east of China. *Chinese Science Bulletin*, **48**(19): 2094—2100

Mao J T, Li C C, Zhang J H, Liu X Y and Liu Q H. 2002. The comparison between remote sensing aerosol optical depth from MODIS data and ground sun photometer observations in Beijing area. *Journal of Applied Meteorological Science*, **13**: 127—135

Mi W, Li Z Q, Xia X A, Holben B, Levy R, Zhao F S, Chen H B and Cribb M. 2007. Evaluation of the moderate resolution imaging spectroradiometer aerosol products at two aerosol robotic network stations in China, *J. Geophys. Res.*, **112**, D22S08, doi:10.1029/2007JD008474.

Rao C R N, Stowe L L and McClain E P. 1989. Remote sensing of aerosols over the oceans using AVHRR data: Theory, practice, and applications. *International Journal of Remote Sensing*, **10**: 743—749

Remer L A and Kaufman Y J. 1998. Dynamic aerosol model: Urban/industrial aerosol. *J Geophys. Res.*, **103**(D12): 13859—13871

Remer L A, Kaufman Y J, Tanr D, Mattoo S, Chu D A, Martins J V, Li R R, Ichoku C, Levy R C, Kleidman R G, Eck T F, Vermote E and Holben B N. 2005. The MODIS aerosol algorithm, products and validation. *Journal of the Atmospheric Sciences*, **62**(4): 947—973

Remer L A, Wald A E and Kaufman Y J. 2001. Angular and seasonal variation of spectral surface reflectance ratios: Implications for the remote sensing of aerosol over land. *IEEE Transactions on Geoscience and Remote Sensing*, **39**(2): 275—283

Sheng P X, Mao J T, Li J G, Zhang A C, San J G and Pan N X. 2003. Atmospheric Physics. Beijing: Peking University Press

Veefkind J P, De Leeuw G, Stamnes P and Koelemeijer B A. 2000. Regional distribution of aerosol over land derived from ATSR-2 and GOME data. *Remote Sensing of Environment*, **74**(3): 377—386

Wang L L, Xin J Y, Wang Y S, Li Z Q, Wang P C, Liu G R and Wen T X. 2007. Validation of MODIS aerosol products by CSHNET over China. *Chinese Science Bulletin*, **52** (4): 477—486

Wiscombe W J. 1981. Improved mie scattering algorithms. *Applied Optics*, **19**(9): 1505—1509

Xia X A. 2006. Remarkable overestimate of MODIS aerosol optical thickness over global land. *Chinese Science Bulletin*, **51**(19): 2297—2303

(C)1994-2021 China Academic Journal Electronic Publishing House. All rights reserved. http://www.cnki.net

MODIS 气溶胶 C004、C005 产品的对比分析及其在中国北方地区的适用性评价

周春艳[1,2], 柳钦火[1], 唐　勇[1], 王　凯[1], 孙　林[3], 何颖霞[4]

1. 遥感科学国家重点实验室, 中国科学院 遥感应用研究所, 北京 100101;
2. 国家环保部卫星环境应用中心, 北京 100029;
3. 山东科技大学 测绘学院, 山东 青岛 266510;
4. 临沂市环境监测站, 山东 临沂 276000

摘　要: 详细介绍了 MODIS 气溶胶 C005 产品算法的改进情况。选择北京、榆林为试验区, 利用 AERONET 地基观测的气溶胶光学厚度数据, 对比分析了上午星 TERRA、下午星 AQUA 的 MODIS 气溶胶 C004、C005 新旧产品的精度, 评价了它们在中国北方地区的适用性。采用波长插值、时空匹配将地基数据和 MODIS 气溶胶产品匹配在一起, 然后采用线性拟合的方法进行对比分析。文中就 MODIS 气溶胶产品和地基数据的时空匹配, 摒弃了 NASA 关于 MODIS 气溶胶产品在全球所采用的方法, 引入当地月平均风速, 提出了中国北方地区时空匹配尺度。对比分析以及评价结果表明: (1) C005 产品算法的改进并没有提高北京站点气溶胶光学厚度的精度, 在 AOT<0.8 时反而是下降的; C004、C005 产品在北京站点不具有显著适用性, 但 C004 比 C005 产品效果好。(2) 榆林站点, TERRA-MODIS C004 产品能够达到需求标准, 而 AQUA-MODIS C004 精度有所下降; 两星的 C005 产品精度较 C004 有很大程度的改善, 470、550、660nm 3 个波段的气溶胶光学厚度与 AERONET 地基观测数据的相关系数均高于 0.9, 具有显著适用性。这说明了新算法所采用的确定地表反射率的方法在植被覆盖好的地区是可行的, 在高反射地区效果不好。

关键词: MODIS, C005, AERONET, 气溶胶光学厚度, 验证

中图分类号: P407　　文献标识码: A

1 引　言

大气气溶胶是指悬浮在大气中的固体和液体微粒与气体载体共同组成的多相体系(盛裴轩等, 2003)。气溶胶的来源主要有人工源和自然源两大类。人工源为人类活动所产生, 主要来自化石燃料的燃烧、工农业生产活动等; 自然源为自然现象所产生, 土壤和岩石的风化, 森林火灾与火山爆发所产生的大量的烟尘颗粒和微尘, 海洋上的浪花碎末进入大气等。大气气溶胶是大气中重要的成分之一, 具有分布广泛、生命期短暂、空间变化迅速、化学组成复杂等特性, 对全球和区域气候变化、大气环境质量具有重要的作用和影响, 已成为当前大气科学研究的重要领域之一(Houghton 等, 1995; Anderson 等, 2003)。

目前, 探测大气气溶胶的方法有地基观测和卫星遥感探测两种。地基观测可以准确提供空间某点的气溶胶光学厚度信息, 但由于观测条件、仪器设备等条件所限, 地基观测不能在空间范围内得到广泛扩展。卫星遥感克服了地基观测空间上的不足, 可以提供全球范围内气溶胶特性数据。卫星遥感探测气溶胶的研究始于 20 世纪 70 年代中期, 为了获取气溶胶光学特性的全球分布、气溶胶直接强迫和间接强迫的季节和年变化, 国际上实施了一系列卫

收稿日期: 2008-04-14; 修订日期: 2008-05-14

基金项目: 中国科学院知识创新工程重要方向性项目(编号: KZCX2-YW-313)和国家自然科学基金重点项目(编号: 40730525)。

第一作者简介: 周春艳(1981—), 女, 2009年7月于中国科学院遥感应用研究所获理学博士学位。现从事大气气溶胶和水汽卫星遥感反演方面的研究。E-mail: mezhouchunyan@126.com。

通讯作者: 柳钦火, E-mail: Qhliu@irsarac.cn。

(C)1994-2021 China Academic Journal Electronic Publishing House. All rights reserved. http://www.cnki.net

星观测计划, 包括: NOAA/AVHRR(Rao 等, 1989)、TOMS(Herman 等, 1997)、ATSR-2(Veefkind 等, 2000)、POLDER(Deuze 等, 1993)、MODIS(Kaufman 等, 1997a)等。

MODIS 是搭载于平台 EOS-AM1/TERRA 和 EOS-PM1/AQUA 太阳同步极地轨道系列卫星上的中分辨率成像光谱仪。它具有 36 个波段, 光谱范围宽, 从 0.4—14.4μm 全光谱覆盖。MODIS 气溶胶产品首次给出覆盖全球的高空间分辨率的气溶胶光学特性资料, 目前已达到一定精度, 可用于气候模型的计算、环境污染动态变化分析和空气质量监测等, 在全球范围内得到了广泛应用(Ichoku 等, 2004)。过去 10 年, MODIS 气溶胶产品算法经历了多次更新, 2006 年又推出了最新版本的气溶胶产品 Collection 005, 以取代 Collection 004(Levy 等, 2007)。近年来, 越来越多的科研人员开始利用 MODIS 气溶胶产品研究中国地区的气溶胶特性, 利用地基观测数据对 MODIS 气溶胶产品进行评价是最基础的研究。毛节泰等(2002)利用北京大学地基太阳光度计资料验证了北京地区 MODIS 卫星遥感气溶胶产品的精度。提取距离地基站点 15 km 范围内最近的 MODIS 像元值, 与 1h 内的地基太阳光度计数据进行比较分析。由于地基观测的限制, 导致两者时间上存在差异, 验证过程进行了空间和时间的约束。李成才等(2003)利用北京和香港地区地基太阳光度计资料确认了两地 NASA TERRA 卫星的 MODIS 气溶胶产品的精度, 然后利用 MODIS 气溶胶产品统计了中国东部地区气溶胶光学特性和季节变化特点。夏祥鳌(2006)对比了 AERONET 和 MODIS 陆地上空气溶胶光学厚度资料, 表明在全球大部分地区 MODIS 高估了气溶胶光学厚度。王莉莉等(2007)利用中国地区太阳分光观测网(CSHNET)气溶胶光学厚度地基联网数据, 评估了 MODIS 气溶胶光学厚度产品在中国不同生态类型和地理区域的适用性。Mi 等(2007)利用香河和太湖两个地基站点评估了 MODIS 在中国地区的精度。其中, 上面所述李成才等、夏祥鳌、王莉莉等、Mi 等在研究过程中, 均采用 NASA 关于 MODIS 气溶胶产品在全球陆地上空的验证方法, 即选取以站点为中心 50 km×50 km 范围内 MODIS 产品数据的空间平均与卫星过境前后 0.5 h 的 AERONET 地基数据的时间平均进行比较。这种方法具有宏观性, 是全球尺度上的, 就局部地区而言, 并不准确。本文在充分考虑中国地区气溶胶移动速度的基础上, 利用 NASA 在全球建立的地面太阳光度计观测网, 验证评价 MODIS 新旧版本气溶胶产品在中国地区的适用性。

2 MODIS 陆地气溶胶 C005 产品算法

到目前为止, 上午星 TERRA 的 MODIS 气溶胶产品经历了 Collection002, 003, 004, 005(简称 C002、C003, C004, C005)4 次更新, C002 是第一版本的业务化产品, 主要用来验证和分析, 没有得到广泛推广应用。C003, C004 数据产品进行了发布, 并得到了广泛的应用。下午星 AQUA 的 MODIS 气溶胶产品经历了 C003, C004, C005 三次更新, 其算法与相同版本的 TERRA-MODIS 的算法大致相同, 只进行细微的补充(Levy 等, 2007)。MODIS 气溶胶 C005 产品是 2006 年下半年发布的, 此次产品升级对 C004 产品算法作了很大的改进(Levy 等, 2007; Ichoku 等, 2005)。本文从 3 个方面介绍气溶胶 C005 产品算法的重要改进。

2.1 反演思想的变化

气溶胶 C004 产品反演算法假设气溶胶在 2.12μm 波段对大气没有散射和吸收, 即 2.12μm 波段的表观反射率等于地表真实反射率。气溶胶 C005 产品算法认为这个假设不成立, 很多研究表明 2.12μm 波段处粗模式气溶胶具有不可忽视的影响(Levy 等, 2007)。

陆地气溶胶 C004 产品反演算法采用 Kaufman 等(1997b)中提出的假设, 即在绿色植被、黑色土壤等暗目标地区, 2.12μm 波段地表反射率与可见光红波段、蓝波段地表反射率之间存在固定的线性关系, 即 0.47μm 的地表反射率等于 2.12μm 地表反射率的 1/4, 而 0.66μm 的地表反射率等于 2.12μm 地表反射率的 1/2。随后很多研究发现可见光波段与近红外波段地表反射率的比值是随着散射几何条件发生变化的, 在很多观测条件下不满足 Kaufman 等(1997b)提出的关系(Remer 等, 2001; Gatebe 等, 2001), 从而 Kaufman 等(1997b)提出的假设被完全打破。鉴于这些发现, 气溶胶 C005 产品反演算法采用了新的反演思想: 在暗目标地区, 可见光红波段与近红外波段地表反射率的关系是散射角和植被指数的函数, 可见光红波段与蓝波段地表反射率有固定的线性关系。具体描述如下(Levy 等, 2007):

$$\rho^{s}_{0.66} = f(\rho^{s}_{2.12}) = \rho^{s}_{2.12} \times \mathrm{slope}_{0.66/2.12} + \mathrm{yint}_{0.66/2.12}$$

$$\rho^{s}_{0.47} = f(\rho^{s}_{0.66}) = \rho^{s}_{0.66} \times \mathrm{slope}_{0.47/0.66} + \mathrm{yint}_{0.47/0.66}$$

其中,

(C)1994-2021 China Academic Journal Electronic Publishing House. All rights reserved. http://www.cnki.net

$$\text{slope}_{0.66/2.12}=\text{slope}_{0.66/2.12}^{\text{NDVI}_{\text{SWIR}}}+0.002\Theta-0.27,$$

$$\text{yint}_{0.66/2.12}=-0.00025\Theta+0.033,$$

$$\text{slope}_{0.47/0.66}=0.49,$$

$$\text{yint}_{0.47/0.66}=0.005.$$

$$\text{slope}_{0.66/2.12}^{\text{NDVI}_{\text{SWIR}}}=0.48;\ \text{NDVI}_{\text{SWIR}}<0.25,$$

$$\text{slope}_{0.66/2.12}^{\text{NDVI}_{\text{SWIR}}}=0.58;\ \text{NDVI}_{\text{SWIR}}>0.75,$$

$$\text{slope}_{0.66/2.12}^{\text{NDVI}_{\text{SWIR}}}=0.48+0.2(\text{NDVI}_{\text{SWIR}}-0.25);$$

$$0.25\leqslant\text{NDVI}_{\text{SWIR}}\leqslant 0.75.$$

$$\text{NDVI}_{\text{SWIR}}=(\rho^{\text{m}}_{1.24}-\rho^{\text{m}}_{2.12})/(\rho^{\text{m}}_{1.24}+\rho^{\text{m}}_{2.12}).$$

$\rho^{\text{s}}_{0.66}$, $\rho^{\text{s}}_{0.47}$, $\rho^{\text{s}}_{2.12}$ 分别表示 0.66, 0.47, 2.12μm 波段的地表反射率; $\rho^{\text{m}}_{1.24}$, $\rho^{\text{m}}_{2.12}$ 分别表示 1.24, 2.12μm 波段的观测反射率; Θ表示散射角。

2.2 辐射传输方程的变化

气溶胶 C004 产品反演算法构建查找表采用 SPD 这种标量辐射传输方程(Dave, 1970)。Fraser 等(1992)、Levy 等(2004)研究发现在某些观测条件下, 忽略散射的偏振信息会导致表观反射率极大的误差。气溶胶 C005 产品反演算法采用了 RT3 偏振辐射传输方程(Evans & Stephens, 1991), 在实际使用过程中可以选择考虑或不考虑偏振信息, 便于跟旧版本进行衔接。另外, 还采用 MIEV 米散射(Wiscombe, 1981)、T-matrix(Dubovik 等, 2002a)代码分别用于计算球形和椭球形粒子气溶胶散射相函数的参数, 作为 RT3 的输入(Levy 等, 2007)。

2.3 气溶胶模式的变化

气溶胶C005产品反演算法根据地理分布, 对气溶胶模式进行了更新。对 Dubovik 等, (2002b)研究结果作了微调, 确定了 5 种气溶胶模式, 分别是大陆型、尘埃型、非吸收型、中度吸收型和严重吸收型。这与以前版本中所使用的气溶胶模式有很大差异, 以前版本中的气溶胶模式是基于 Remer 等 1998 年的研究结果。大陆型气溶胶模式只用于地表较亮的特殊情况; 非吸收型、中度吸收型、严重吸收型属于细模式, 随季节和地理位置的变化而变化; 气溶胶 C005 产品反演算法选择尘埃型和 3 种细模式中的一个进行组合定义气溶胶类型(Levy 等, 2007)。

气溶胶 C005 产品反演算法根据 AERONET 地基观测数据, 重新定义了气溶胶的光学特性参数, 尤其是单次散射反照率(SSA): 非吸收型 SSA~0.95, 中度吸收型 SSA~0.90, 严重吸收型 SSA~0.85(Levy 等, 2007)。在中国, 除了东部沿海, 大部分地区被定义为中度吸收型气溶胶。因为 AERONET 站点在全球分布不均, 中国地区过去几年站点稀疏, 导致气溶胶光学特性的研究不够深入。随着大气气溶胶地基观测技术被越来越多的人掌握, 近年来中国 AERONET 站点有明显的增加, 很多省市级单位开始了自主观测。中国科学院大气物理研究所构建了中国地区太阳分光观测网(CSHNET), 观测网目前有 19 个中国生态系统研究网络(CERN)生态观测站、4 个城市观测点、2 个标定中心和 1 个数据中心。中国科学院遥感应用研究所为监测 2008 年奥运会期间奥运场馆附近大气状况, 在研究所楼顶安置了 CE318 太阳分光光度计。河北省、山西省等省市开始利用 CE318 太阳分光光度计进行大气气溶胶的观测。

气溶胶C005产品反演算法还做了许多修正, 如暗目标的选择方法、云掩模方法、雪掩模方法、中心波长的定义、高程的修正方法等(Levy 等, 2007)。

3 中国地区气溶胶光学厚度产品的验证方案设计

3.1 验证数据准备

本文收集到 2002 年 8 月 28 日至 10 月 8 日覆盖中国北部地区的 TERRA\AQUA-MODIS C004 Level 2、TERRA\AQUA-MODIS C005 Level 2 气溶胶产品, 同时也收集到同一时间段内的 AERONET 地基观测的气溶胶光学厚度数据, 当时中国北部地区只有北京、榆林两个地基站点。本文利用北京、榆林两个 AERONET 站点数据对上午星 TERRA、下午星 AQUA 的 MODIS 气溶胶光学厚度 C004、C005 产品进行验证评价。

AERONET 是由美国国家宇航局 NASA 和法国国家科学研究中心 CNRS 共同建立的一个地基气溶胶遥感网络。此计划提供全球具有代表性区域的气溶胶光学特性参数, 用于研究全球气溶胶的传输、辐射效应, 验证辐射传输模式和卫星反演的气溶胶光学特性参数的精度。它是当前世界上正在业务运行的一个大型气溶胶观测网络, 在世界各地分布有大量的观测站点, 整个网络统一采用法国 CIMEL 公司开发生产的多波段太阳光度计进行观测, 实现了仪器、定标、数据处理和数据分发的标准化, 观测数据精度很高, 目前已广泛应用于气溶胶光学特性精度的验证。AERONET 提供 3 个质量等级的气溶胶光学厚度数据: Level 1.0, 未经过严格滤云和最后验证的数据; Level 1.5, 经过严格滤云但没有最后验证的数据; Level 2.0, 经过严格滤云和最后验证、有质量保证的数据(Holben 等, 1998)。本文采用 Level

(C)1994-2021 China Academic Journal Electronic Publishing House. All rights reserved. http://www.cnki.net

2.0 AERONET 气溶胶光学厚度数据对 MODIS 气溶胶产品进行验证。

3.2 数据匹配方法

由于 MODIS 和 AERONET 对气溶胶观测的中心波长和时空尺度不同，为了使两者具有可比性，需要对气溶胶光学厚度数据作波长差值和时空匹配处理(陈本清等, 2005)。

3.2.1 AERONET 数据的波长插值计算

AERONET 一般可提供 1020、870、670、500、440、380、340nm 波段的气溶胶光学厚度，而 MODIS 提供 470、550、660nm 3 个波段的气溶胶产品，两者没有相对应的波段，因此需要对 AERONET 数据进行波长插值计算，得到与 MODIS 相匹配波段的气溶胶光学厚度。本文将通过 440、870nm 两个波段的气溶胶光学厚度插值得到 470、550、660nm 3 个波段的数值。AERONET 500nm 不参与插值，是为了保证验证具有普遍性，因为并不是所有的 AERONET 站点都有 500nm 波段。AERONET 有 670nm 波段的观测，与 MODIS 660nm 差别不大，为了保证此波段与其他两波段一样不受波段偶然校准误差的影响，本文仍然采用两波段的插值计算得到 AERONET 660nm 波段数值(Fraser 等,1992; Remer 等, 2005)。

在没有水汽影响的波段上，气溶胶粒子的谱分布满足 Junge 分布，气溶胶光学厚度跟波长之间满足 Angstrom 关系式(Angstrom,1964):

$$\tau_a(\lambda) = \beta\lambda^{-\alpha}$$

式中，$\tau_a(\lambda)$表示波长λ的气溶胶光学厚度；β表示 Angstrom 浑浊度系数，与气溶胶粒子总数、粒子谱分布和折射指数有关；α表示 Angstrom 波长指数，与气溶胶的平均半径有关，取值为[0, 4]，气溶胶粒子越大，α值越小。

设波段λ_1、λ_2没有水汽影响，则有:

$$\tau_a(\lambda_1) = \beta\lambda_1^{-\alpha}$$

$$\tau_a(\lambda_2) = \beta\lambda_2^{-\alpha}$$

由上面两式可得:

$$\alpha_{870/440} = -\frac{\ln(\tau_a(870)/\tau_a(440))}{\ln(870/440)}$$

470、550、660nm 3 个波段的气溶胶光学厚度值可以分别用下式求得:

$$\tau_a(\lambda) = \tau_a(870)(\lambda/870)^{-\alpha_{870/440}}$$

数据插值的误差介于 0—10%，这取决于气溶胶类型的不同。细模式占主导的气溶胶类型光学厚度大时误差最大，混合模式或者是粗模式气溶胶类型误差最小(Eck 等, 1999)。

3.2.2 MODIS 数据与 AERONET 数据的时空匹配

AERONET 地基观测的气溶胶光学厚度是空间上某些点间隔固定时间的连续观测，MODIS 气溶胶光学厚度是空间上以 10km×10km 为观测单元的面上瞬时观测。本文采用 TERRA、AQUA 两星产品数据参与分析，TERRA 过境时间大约为当地时间上午 10:30, AQUA 过境时间大约为下午 2:30。MODIS 与 AERONET 观测的时空尺度不同，如果简单的取 MODIS 卫星过境时间点的 AERONET 地基数据与单个 MODIS 像元值对比，就是拿空间一点的气溶胶光学厚度与 10km×10km 空间范围的气溶胶光学厚度的均值作比较，这种比较缺乏可信度，需要寻找一种稳定可靠的匹配方法。目前普遍采用的方法是 NASA 关于 MODIS 气溶胶产品在全球陆地上空的验证方法，选取以站点为中心 50 km×50 km 范围内 MODIS 产品数据的空间平均与卫星过境前后 0.5h 的 AERONET 地基数据的时间平均进行匹配，这种匹配方法是基于全球尺度上大气气溶胶的平均移动速度为 50km/h 的假设(Ichoku 等, 2002)。在区域尺度上，这种假设并不准确。

大气气溶胶的运动速度受多种因素的影响，水平方向上受风速的影响，垂直方向上受湍流的影响，在此只考虑其水平方向的运动。根据中国气象科学数据共享服务网(中国气象局国家气象信息中心, 2008)提供的气候背景数据统计资料，中国北京、榆林站点 1971—2000 年月平均风速如表 1。以北京站点为例，3 个月风速相差不大，考虑到文中所用数据大多是 9 月份的，所以就采用 9 月份的风速, 1h 风的运行距离是 7.2km，风是气溶胶的运动载体，我们认为气溶胶的运行速度也是 7.2km/h。榆林地区的为 6.48km/h。考虑到 MODIS 气溶胶产品的最小单元是 10km×10km，所以本文将利用 MODIS 一个像素的气溶胶光学厚度数值与 MODIS 过境前后 0.5h 内的 AERONET 站点数据的平均进行比较分析。

表 1 研究站点风速/(m/s)

月份 / 站点	8 月	9 月	10 月
北京	1.8	2.0	2.1
榆林	2.2	1.8	1.8

3.3 验证方法

经过对 AERONET 数据进行波长插值，并与 MODIS 数据进行时空匹配后，现对两者进行线性拟合分析:

$$\tau_{\mathrm{MODIS}} = A\tau_{\mathrm{AERONET}} + B$$

(C)1994-2021 China Academic Journal Electronic Publishing House. All rights reserved. http://www.cnki.net

式中, τ_{MODIS} 为 MODIS 产品的气溶胶光学厚度; A 为斜率; $\tau_{AERONET}$ 为 AERONET 地基观测的气溶胶光学厚度; B 为截距。

在理想情况下, MODIS 的气溶胶光学厚度与 AERONET 地基观测的气溶胶光学厚度应该一致, 即: A=1, B=0, 相关系数 R=1。实际上, 由于观测仪器自身因素、波长插值、时空匹配, 当然最主要原因是 MODIS 气溶胶反演带来的误差, 使得两者存在一定差异。本文通过拟合方程的线性相关系数 R、斜率 A、截距 B 以及表 2 和表 3 所列的 MODIS 产品数据落入期望误差范围的概率来评价 MODIS 的气溶胶光学厚度的精度。

4 结果与分析

图 1 和图 2 分别给出了北京、榆林两站点上午

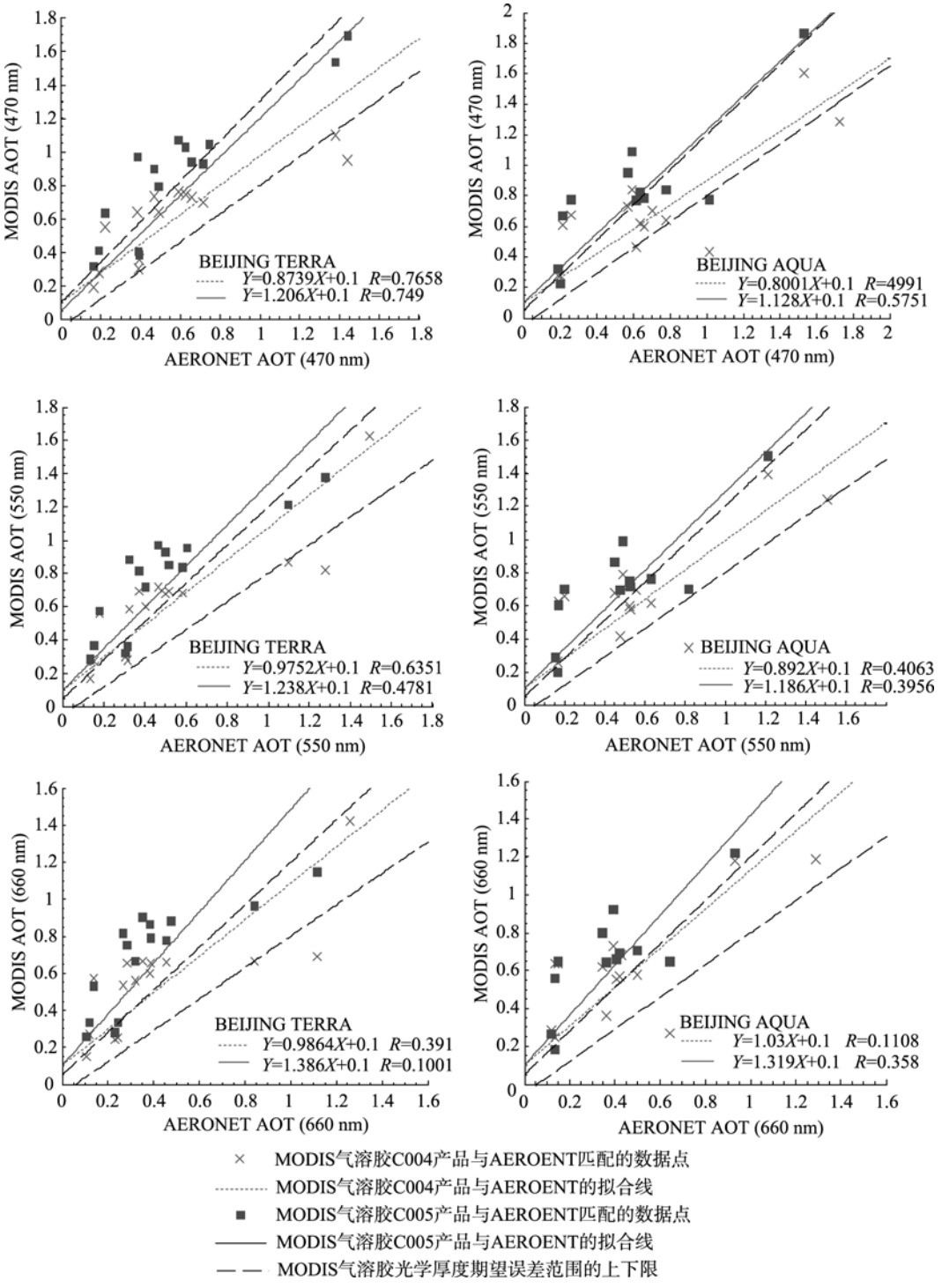

图 1 北京站点 TERRA(左)、AQUA(右)的 MODIS 470nm(上)、550nm(中)、660nm(下)3 个波段气溶胶光学厚度与 AERONET 地基观测的气溶胶光学厚度的线性拟合结果

(C)1994-2021 China Academic Journal Electronic Publishing House. All rights reserved. http://www.cnki.net

表 2 北京站点 TERRA、AQUA 的 MODIS 气溶胶光学厚度满足 NASA 期望误差范围的概率统计

波长	470nm		550nm		660nm	
产品名称	C004	C005	C004	C005	C004	C005
TERRA/%	46.7	26.7	33.3	26.7	26.7	20.0
AQUA/%	42.9	25.0	42.9	25.0	21.4	16.7

星 TERRA、下午星 AQUA 的 MODIS 470、550、660nm 3 个波段气溶胶光学厚度与 AERONET 地基观测的气溶胶光学厚度的线性拟合结果。采用平面坐标系, 以 AERONET 地基观测数据为横坐标, 以 MODIS 的气溶胶光学厚度为纵坐标。MODIS 气溶胶光学厚度期望误差范围的上下限, 本文采用 NASA 定义的陆地上空 MODIS 气溶胶光学厚度产品的期望误差范围 $\tau=\pm0.05\pm0.15\tau_{AERONET}$(Remer 等, 2005)。图 1 和图 2 中给出了 MODIS 气溶胶产品与 AERONET 数据的线性拟合方程和相关系数 R。

图 1 左栏, 为北京站点 TERRA-MODIS 470、550、660nm 3 个波段气溶胶光学厚度与 AERONET 地基观测的气溶胶光学厚度的线性拟合结果。本文选择的数据中, 北京站点 TERRA-MODIS C004、C005 均有 26 个有效值, 但能够与 AERONET 地基数据匹配的只有 15 个, 导致匹配数据较少的一个很重要的原因是 10 月 1—7 日北京站点地基数据缺失。直观分析 470、550、660nm 3 个波段的拟合结果, 发现: 在 AERONET AOT<0.8 时, 值 C004 大多低于 C005, 但两者明显高估了真实光学厚度; 当 AERONET AOT>0.8 时, C004 严重低估了真实值, 而 C005 能够较为准确地反映真实值。470 nm 波段(图 1 左上), C004、C005 气溶胶光学厚度与 AERONET 气溶胶光学厚度的线性拟合方程斜率分别为 0.8739、1.206, 截距都为 0.1, 相关系数分别为 0.7658、0.749, 满足 NASA 的期望误差的数据样点分别为 46.7%、26.7%(表 2)。这些数据表明 470nm 波段上 C004 产品的精度高于 C005 产品, 但是两种产品与真值的拟合效果均不好, 满足期望误差的样本点数较低, 因此它们在北京站点的适用性较差。通过分析 550、660nm 波段拟合方程的斜率、截距、相关系数以及满足期望误差样点数 4 个指标, 得出与 470nm 波段相似的结论: TERRA-MODIS 气溶胶 C004、C005 产品在北京地区不具有显著适用性, 但 C004 比 C005 产品精度高。

图 1 右栏, 为北京站点 AQUA-MODIS 470、550、660nm 3 个波段气溶胶光学厚度与 AERONET 地基观测的气溶胶光学厚度的线性拟合结果。在 MODIS 气溶胶产品的验证中, 人们往往忽视了 AQUA-MODIS 数据。AQUA 大约当地时间下午 2:30 过境, 与此同时 AERONET 数据也比较丰富, 可以对它进行分析。在本文选择的数据中, 北京站点 AQUA-MODIS C004 有 24 个有效数据, 而 C005 只有 20 个, 这是 C005 对云检测更加严格所造成的。与 AERONET 匹配后, C004、C005 分别有 14、12 个有效数据参与拟合。通过图 1 右栏所示 3 个波段的拟合公式看出: 3 个波段的 AQUA-MODIS 气溶胶产品数据与 AERONET 拟合效果很差, 截距高达 0.1, 斜率也远远偏离 1, 相关系数除了 C005 的 470nm 达到 0.5751 外, 其他波段均较低。满足 NASA 的期望误差的数据样点数比 TERRA 有所下降(表 2)。北京站点的 AQUA-MODIS 气溶胶产品数据不具有适用性, 比 TERRA 产品精度更差, 这是两颗卫星系统误差不同造成的。

北京站点(39.977N, 116.381E)安置在中国科学院大气物理研究所内楼顶上, 方圆 1km 内是居民楼、商业房、马路等, 成规模的植被覆盖少, 只有零星的绿化带。这一站点属于典型的城市型气溶胶。通过对北京站点 TERRA、AQUA 两颗卫星的 MODIS 气溶胶 C004、C005 产品进行验证分析可知, C004、C005 产品不具有显著适用性, 但 C004 比 C005 产品效果要好; C005 产品算法的改进并没有提高北京站点气溶胶光学厚度的精度, 在 AOT<0.8 的时候反而是下降的。C005 产品与真值的显著性差异首要原因是算法不能准确确定城市这种高反射地表的反射率。MODIS C005 产品算法确定地表反射率的方法是寻找暗目标, 而北京站点附近没有成规模的植被覆盖, 另外本文研究的数据是秋天, 这导致算法很难找到暗目标, 从而无法准确确定地表反射率。另外, 北京地区的气溶胶属于人工源, 供暖、烹调燃煤、燃气或燃油排放大量烟尘, 汽车等交通工具排放尾气, 这种气溶胶特性难以准确描述。这也是气溶胶光学厚度得不到准确反映的一个很重要的原因。总之, MODIS C004、C005 产品对高反射地表不具有适用性。

图 2 左栏: 为榆林站点 TERRA-MODIS 470、550、660nm 3 个波段气溶胶光学厚度与 AERONET 地基观测的气溶胶光学厚度的线性拟合结果。本文

(C)1994-2021 China Academic Journal Electronic Publishing House. All rights reserved. http://www.cnki.net

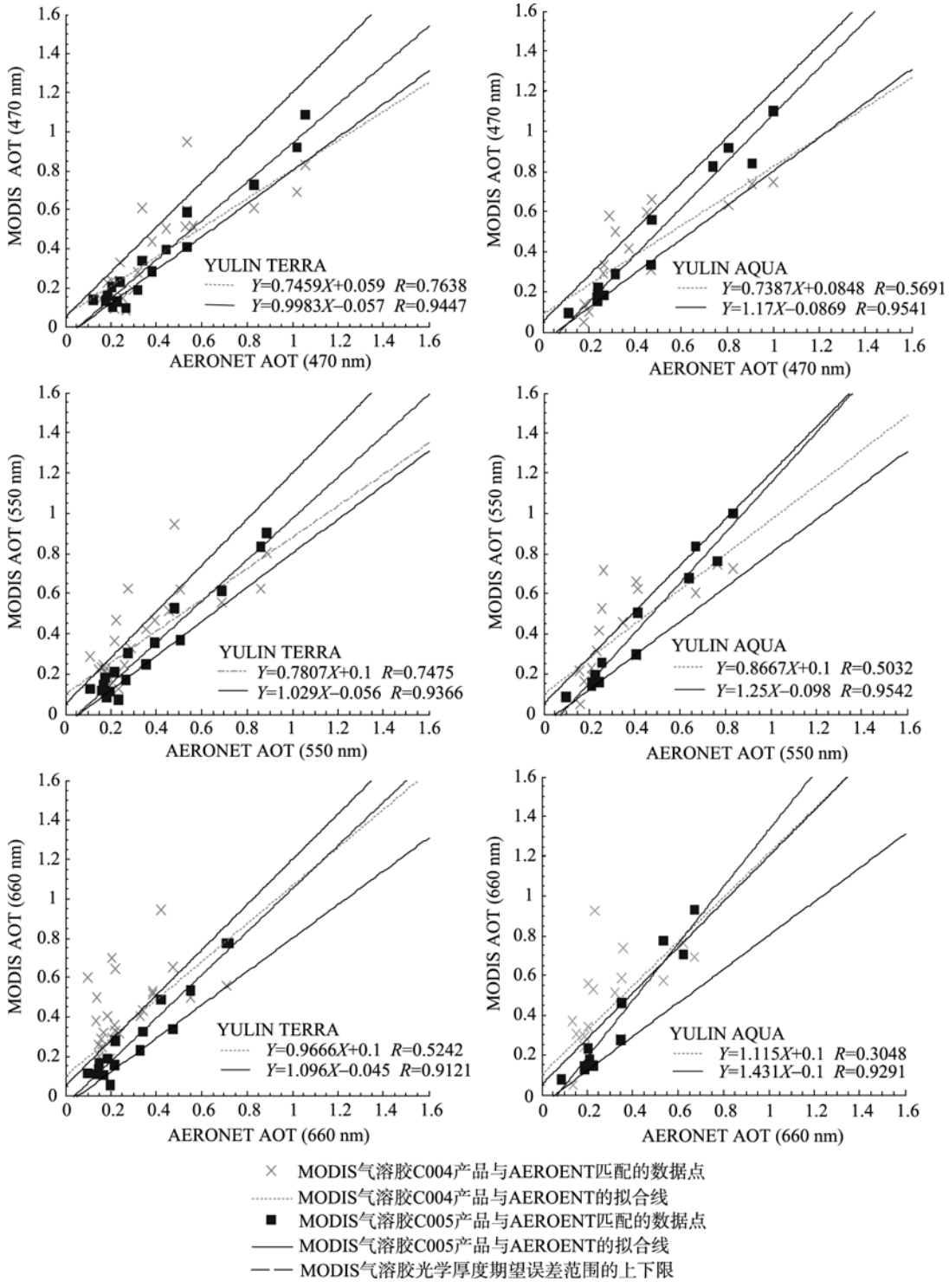

图 2　榆林站点 TERRA(左)、AQUA(右)MODIS 470nm(上)、550nm(中)、660nm(下)3 个波段的气溶胶光学厚度与 AERONET 地基观测的气溶胶光学厚度的线性拟合结果

表 3　榆林站点 **TERRA、AQUA MODIS** 的气溶胶光学厚度产品满足 **NASA** 期望误差范围的概率统计

波长	470nm		550nm		660nm	
产品名称	C004	C005	C004	C005	C004	C005
TERRA/%	52.0	76.5	68.0	64.7	32.0	87.5
AQUA/%	43.8	91.7	50.0	75.0	31.3	72.7

(C)1994-2021 China Academic Journal Electronic Publishing House. All rights reserved. http://www.cnki.net

选择的数据中，榆林站点 TERRA-MODIS C004、C005 分别有 26、18 个有效数据。与 AERONET 匹配后, C004、C005 分别有 25、17 个有效数据参与拟合。470nm 波段(图 2 左上), C005 拟合方程的斜率为 0.9983，很接近于 1，相关系数也高达 0.9447，满足误差范围的样本数达到 76.5%(表 3)，比 C004 数据精度有很大提高。550nm 波段(图 2 左中), C005 拟合方程斜率接近 1，截距为–0.056，相关系数保持在 0.9366，有 64.7%的样本满足误差要求，仍然保持很高的精度；C004 这一波段相关系数有所下降，截距高达 0.1，但是落入误差范围的样点数有所提高，达到 68.0%。这一波段的 C004、C005 产品精度都有可信性，但 C005 产品精度达到很高的水平。660nm 波段(图 2 左下)，C005 拟合方程各项系数依然很理想，满足误差要求的样本数提高到 87.5%，产品精度值得信赖；C004 的相关系数降低到 0.5242，满足误差要求的样本数下降到 32.0%，相比其他两个波段，产品精度大幅下降。总之，对 C004 而言，470nm 波段精度最好，其次 550nm，再次 660nm，前两个波段产品具有可信性；对 C005 而言，三个波段产品精度相差不大，都保持在很高的水平，具有显著适用性。

图 2 右栏：为榆林站点 AQUA-MODIS 470、550、660nm 3 个波段气溶胶光学厚度与 AERONET 地基观测的气溶胶光学厚度的线性拟合结果。与 AERONET 时间匹配后, C004 有 16 个有效数据，而 C005 只有 12 个。综合考虑 470、550、660nm 波段线性拟合方程的斜率、截距、相关系数以及样本落入期望误差范围的概率(表 3)可知, AQUA C005 产品精度如 TERRA C005 一样保持很高的水平，唯一的差别是 AQUA 拟合方程的斜率变大; AQUA C004 的相关系数较 TERRA 有很大程度的下降，满足误差要求的样本数也有不同程度的下降。在榆林地区，AQUA C005 产品具有显著适用性。

榆林站点(38.283N，109.717E)安置在陕西省榆林市陕西沙漠研究所楼顶，高程约 1080m。榆林地区，春季多风沙、夏季多雨，夏秋季节植被覆盖好，天气状况较好。通过上述比较分析可知，榆林站点 TERRA-MODIS C004 产品能够达到需求标准，而 AQUA-MODIS C004 精度有所下降；两星的 C005 产品精度都达到了很高的水平，具有显著适用性。C005 产品算法关于地表反射率的确定方法的改进，在植被覆盖好的地方效果非常显著，榆林站点的气溶胶光学厚度精度得到了显著提高。

5 结 论

本文利用北京、榆林两个 AERONET 地基观测站点数据对双星的 MODIS C004、C005 两种产品的气溶胶光学厚度数据进行了对比分析，得出如下结论：(1) C005 产品算法的改进并没有提高北京站点气溶胶光学厚度的精度，在 AOT<0.8 的时候反而是下降的；C004、C005 产品在北京站点不具有显著适用性，但 C004 比 C005 产品效果好。(2) 榆林站点，TERRA-MODIS C004 产品能够达到需求标准，而 AQUA-MODIS C004 精度有所下降；两星的 C005 产品精度较 C004 有很大程度的改善, 470、550、660nm 3 个波段的气溶胶光学厚度与 AERONET 地基观测数据的相关系数均高于 0.9，具有显著适用性。这说明了新算法所采用的确定地表反射率的方法在植被覆盖好的地区是可行的，在高反射地区效果不好。由此可得如下结论：双星的 C004、C005 产品在中国北方的高反射地区都不具有适用性；TERRA-MODIS C004 在植被覆盖好的地方具有一定可信度，而 AQUA-MODIS C004 精度较 TERRA-MDDIS C004 有所下降，可信度差；双星的 C005 产品在中国北方植被覆盖情况良好的地区精度非常高，具有显著适用性。

中国地表类型复杂，要进一步提高陆地上空气溶胶光学厚度反演精度，首先需要准确确定不同地表类型的反射率，如浓密植被地表、稀疏植被地表、高反射地表、内陆湖水体等。目前，浓密植被反射率的确定有比较成熟的模型，而其他地表类型反射率的准确确定还需要进一步研究。其次，对气溶胶特性的描述也是影响产品精度的一个很重要的因素，包括单次散射反照率、折射指数等，在目前越来越多地基观测数据的支持下，对气溶胶特性进行准确地定量描述将成为可能。

致谢：感谢 NASA GSFC 提供本文所需的 MODIS 产品数据、AERONET 地基观测数据。感谢北京大学宋宇老师对作者所遇问题的热心指导。

REFERENCES

Anderson T L, Charlson R J, Schwartz S E, Knutti R, Boucher O, Rodhe H and Heintzenberg J. 2003. Climate forcing by aerosols—a hazy picture. *Science*, **300**(5622): 1103－1104

Angstrom A. 1964. The parameters of atmospheric turbidity. *Tellus*, **16**: 64－75

Chen B Q and Yang Y M. 2005. Validation of MODIS aerosol opti-

(C)1994-2021 China Academic Journal Electronic Publishing House. All rights reserved. http://www.cnki.net

cal thickness in the Taiwan Strait and its circumjacent sea area. *Acta Oceanologica Sinica*, **27**(6): 170—176

China Meteorological Administration.China Meteorological Data Sharing Service System. Ground observation. < http://cdc.cma.gov.cn/> (1 Mar, 2008)

Dave J V. 1970. Intensity and polarization of radiation emerging from a plane-parallel atmosphere containing mono-dispersed aerosols. *Applied Optics*, **9**(12): 2673—2687

Deuze J L, Breon F M, Deschamps P Y, Devaux C, Herman M, Podaire A and Roujean J L.1993. Analysis of the POLDER (Polarization and Directionality of Earth's Reflectances) airborne instrument. *Remote Sensing of Environment*, **45**(2): 137—154

Dubovik O, Holben B N, Lapyonok T, Sinyuk A, Mishchenko M I, Yang P and Slutsker I. 2002a. Non-spherical aerosol retrieval method employing light scattering by spheroids. *Geophysical Research Letters*, **29**(10): 1415, doi:10.1029/2001GL014506

Dubovik O, Holben B N, Eck T F, Smirnov A, Kaufman Y J, King M D, Tanré D and Slutsker I. 2002b. Variability of absorption and optical properties of key aerosol types observed in worldwide locations. *Journal of the Atmospheric Sciences*, **59**(3): 590—608

Eck T F, Holben B N, Reid J S, Dubovik O, Smirnov A, O'Neill N T, Slutsker I and Kinne S. 1999. Wavelength dependence of the optical depth of biomass burning, urban and desert dust aerosols. *J. Geophys. Res.*, **104**(31): 331—350

Evans K F and Stephens G L. 1991. A new polarized atmospheric radiative transfer model. *Journal of Quantitative Spectroscopy and Radiative Transfer*, **46**(5): 413—423

Fraser R S, Ferrare R A, Kaufman Y J, Markham B L and Mattoo S. 1992. Algorithm for atmospheric corrections of aircraft and satellite imagery. *International Journal of Remote Sensing*, **13**(3): 541—557

Gatebe C K, King M D, Tsay S C, Ji Q, Arnold G T and Li J Y. 2001. Sensitivity of off-nadir zenith angles to correlation between visible and near-infrared reflectance for use in remote sensing of aerosol over land. *IEEE Transactions on Geoscience and Remote Sensing*, **39**(4): 805—819

Herman J R, Bhartia P K, Torres O, Hsu C, Seftor C and Celarier E. 1997. Global distribution of UV-absorbing aerosols from Nimbus 7/TOMS data. *J. Geophys. Res.*, **102**(D14): 16911—16922

Holben B N, Eck T F, Slutsker I, Tanré D, Buis J P, Setzer A, Vermote E, Reagan J A, Kaufman Y J, Nakajima T, Lavenu F, Jankowiak I and Smirnov A. 1998. AERONET-a federated instrument network and data archive for aerosol characterization. *Remote sensing of environment*, **66**(1): 1—16

Houghton J T, Meira Filho L G, Bruce J, Lee H, Callander B A, Haites E, Harris N and Maskell K. 1995. IPCC, Climate Change 1994: Radiative Forcing of Climate Change and an Evaluation of the IPCC IS92 Emission Scenarios. Cambridge: Cambridge University Press

Ichoku C, Chu D A, Mattoo S, Kaufman Y J, Remer L A, Tanré D, Slutsker I and Holben B N. 2002. A spatio-temporal approach for global validation and analysis of MODIS aerosol products. *Geophysical Research Letters*, **29**(12), 8006, doi: 10.1029/2001GL013206.

Ichoku C, Kaufman Y J, Remer L A and Levy R. 2004. Global aerosol remote sensing from MODIS. *Advances in Space Research*, **34**(4): 820—827

Ichoku C, Remer L A and Eck T F. 2005. Quantitative evaluation and intercomparison of morning and afternoon Moderate Resolution Imaging Spectroradiometer (MODIS) aerosol measurements from Terra and Aqua. *J. Geophys. Res.*, **110**, D10S03, doi: 10.1029/2004JD004987.

Kaufman Y J, Tanré D, Remer L A, Vermote E F, Chu A and Holben B N. 1997a. Operational remote sensing of tropospheric aerosol over land from EOS-Moderate Resolution Imaging Spectroradiometer. *J. Geophys. Res*, **102**(D14): 17051—17067

Kaufman Y J, Wald A E, Remer L A, Gao B C, Li R R and Flynn L. 1997b. The MODIS 2.1-um channel–correlation with visible reflectance for use in remote sensing of aerosol. *IEEE Transactions on Geoscience and Remote Sensing*, **35**(5): 1286—1298

Levy R C, Remer L A and Kaufman Y J. 2004. Effects of neglecting polarization on the MODIS aerosolretrieval over land. *IEEE Transactions on Geoscience and Remote Sensing*, **42**(11): 2576—2583

Levy R C, Remer L A, Mattoo S, Vermote E F and Kaufman Y J. 2007. Second-generation operational algorithm: Retrieval of aerosol properties over land from inversion of moderate resolution imaging spectroradiometer spectral reflectance. *J. Geophys. Res.*, **112**, D13211, doi: 10.1029/2006JD007811.

Li C C, Mao J T, Liu Q H, Chen J Z, Yuan Z B, Liu X Y, Zhu A H and Liu G Q. 2003. Study of distribution and the seasonal variation characteristic of aerosol optical thickness using MODIS in the east of China. *Chinese Science Bulletin*, **48**(19): 2094—2100

Mao J T, Li C C, Zhang J H, Liu X Y and Liu Q H. 2002. The comparison between remote sensing aerosol optical depth from MODIS data and ground sun photometer observations in Beijing area. *Journal of Applied Meteorological Science*, **13**: 127—135

Mi W, Li Z Q, Xia X A, Holben B, Levy R, Zhao F S, Chen H B and Cribb M. 2007. Evaluation of the moderate resolution imaging spectroradiometer aerosol products at two aerosol robotic network stations in China, *J. Geophys. Res.*, **112**, D22S08, doi:10.1029/2007JD008474.

(C)1994-2021 China Academic Journal Electronic Publishing House. All rights reserved. http://www.cnki.net

Rao C R N, Stowe L L and McClain E P. 1989. Remote sensing of aerosols over the oceans using AVHRR data: Theory, practice, and applications. *International Journal of Remote Sensing*, **10**: 743—749

Remer L A and Kaufman Y J. 1998. Dynamic aerosol model: Urban/industrial aerosol. *J Geophys. Res.*, **103**(D12): 13859—13871

Remer L A, Kaufman Y J, Tanr D, Mattoo S, Chu D A, Martins J V, Li R R, Ichoku C, Levy R C, Kleidman R G, Eck T F, Vermote E and Holben B N. 2005. The MODIS aerosol algorithm, products and validation. *Journal of the Atmospheric Sciences*, **62**(4): 947—973

Remer L A, Wald A E and Kaufman Y J. 2001. Angular and seasonal variation of spectral surface reflectance ratios: Implications for the remote sensing of aerosol over land. *IEEE Transactions on Geoscience and Remote Sensing*, **39**(2): 275—283

Sheng P X, Mao J T, Li J G, Zhang A C, San J G and Pan N X. 2003. Atmospheric Physics. Beijing: Peking University Press

Veefkind J P, De Leeuw G, Stamnes P and Koelemeijer B A. 2000. Regional distribution of aerosol over land derived from ATSR-2 and GOME data. *Remote Sensing of Environment*, **74**(3): 377—386

Wang L L, Xin J Y, Wang Y S, Li Z Q, Wang P C, Liu G R and Wen T X. 2007. Validation of MODIS aerosol products by CSHNET over China. *Chinese Science Bulletin*, **52** (4): 477—486

Wiscombe W J. 1981. Improved mie scattering algorithms. *Applied Optics*, **19**(9): 1505—1509

Xia X A. 2006. Remarkable overestimate of MODIS aerosol optical thickness over global land. *Chinese Science Bulletin*, **51**(19): 2297—2303

附中文参考文献

陈本清, 杨燕明. 2005. 台湾海峡及周边海区 MODIS 气溶胶光学厚度有效性验证. 海洋学报, **27**(6): 170—176

李成才, 毛节泰, 刘启汉, 陈介中, 袁自冰, 刘晓阳, 朱爱华, 刘桂青. 2003. 利用 MODIS 研究中国东部地区气溶胶光学厚度的分布和季节变化特征. 科学通报, **48**(19): 2094—2100

毛节泰, 李成才, 张军华, 刘晓阳, 刘启汉. 2002. MODIS 卫星遥感北京地区气溶胶光学厚度及与地面光度计遥感的对比. 应用气象学报, **13**: 127—135

盛裴轩, 毛节泰, 李建国, 张霭琛, 桑建国, 潘乃先. 2003. 大气物理学. 北京: 北京大学出版社

王莉莉, 辛金元, 王跃思, 李占清, 王普才, 刘广仁, 温天雪. 2007. CSHNET 观测网评估 MODIS 气溶胶产品在中国区域的适用性. 科学通报, **52**(4): 477—486

夏祥鳌. 2006. 全球陆地上空 MODIS 气溶胶光学厚度显著偏高. 科学通报, **51**(19): 2297—2303

中国气象局国家气象信息中心.China Meteorological Data Sharing Service System. 地面观测. <http://cdc.cma.gov.cn/> (1 Mar, 2008)

(C)1994-2021 China Academic Journal Electronic Publishing House. All rights reserved. http://www.cnki.net